Journal of Solid State Chemistry **164,** 81–87 (2002)
doi:10.1006/jssc.2001.9450, available online at http://www.idealibrary.com on IDEAL®

Hydrothermal Synthesis of the Blue Potassium Molybdenum Bronze, $K_{0.28}MoO_3$

Kin Chin,* Kazuo Eda,* Noriyuki Sotani,*[1] and M. Stanley Whittingham†

**Department of Chemistry, Faculty of Science, Kobe University, Nada-ku, Kobe 657-8501, Japan; and †Institute for Materials Research, State University of New York at Binghamton, Binghamton, New York 13902-6000*

Received July 25, 2001; in revised form October 25, 2001; accepted November 9, 2001

Blue potassium molybdenum bronze, $K_{0.28}MoO_3$, was prepared by hydrothermal heating hydrogen molybdenum bronze in KCl solution at 431 K. Hydrated molybdenum bronze was found formed as an intermediate during the conversion from hydrogen molybdenum bronze to blue bronze. The hydrothermal method proved itself an easy and effective for synthesis of mixed-valence compounds. © 2002 Elsevier Science (USA)

Key Words: **hydrothermal reaction; blue bronze; alkali metal molybdenum bronze; low-temperature synthesis route; hydrated molybdenum bronze; hydrogen molybdenum bronze; mixed-valence compound; topotactical reaction.**

INTRODUCTION

Interest in alkali metal molybdenum bronzes has lasted for decades since their first reported preparation by Wold *et al.* (1) in 1964. They show a wide variety of crystal structures and interesting physical properties, such as low-dimensional metallic behavior (2–4), metal-to-semiconductor transitions driven by charge density wave (5–7), and superconductivity (8). Functional applications are anticipated for high-density storage media, electrochromic devices, electrodes, and so on.

According to the color, stoichiometry, and structure of the compound, alkali molybdenum bronzes can be classified generally into three types: (1) blue bronze, $A_{0.3}MoO_3$ with $A = $ K, Rb, Cs, and Tl; (2) red bronze, $A_{0.33}MoO_3$ with $A = $ Li, K, Rb, Cs, and Tl; (3) purple bronze, $A_{0.9}Mo_6O_{17}$ with $A = $ Li, Na, K, and Tl. Molybdenum bronzes are nonstoichiometric compounds. The theoretical ideal formulas of blue bronze and red bronze are $A_{0.3}MoO_3$ and $A_{0.33}MoO_3$, respectively, while other reduced Mo bronze phases with low alkali metal content are also known.

Alkali metal molybdenum bronzes have been prepared mainly by molten salt methods (1, 9) at temperatures exceeding 800 K: (1) electrolytic reduction of molten mixtures of MoO_3 and A_2MoO_4, and (2) reaction between stoichiometrically mixed A_2MoO_4, MoO_3, and MoO_2. A temperature gradient flux technique was reported by Greenblatt *et al.* (10, 11) in 1984 for the preparation of good-quality single-crystal molybdenum bronzes.

Manthiram *et al.* (12, 13) reported that, after a heat treatment at 623–773 K of the amorphous products formed by the reduction of K_2MoO_4 in KBH_4 solution, $K_{0.26}MoO_3$, $K_{0.30}MoO_3$, and $K_{0.85}MoO_3$ were crystallized with MoO_2. We (14–17) also attained formerly by the solid state reactions a series of alkali metal bronzes containing small amounts of MoO_3 by heating hydrated molybdenum bronzes in the neighborhood of 600 K in N_2 atmosphere.

Recently, we focused our work on the synthesis of alkali metal molybdenum bronzes using hydrothermal methods under mild conditions. Single-phase blue potassium molybdenum bronze was prepared successfully at a temperature of 431 K by the hydrothermal synthesis route we used. Compared with traditional molten salt methods, the formation temperature of alkali metal molybdenum bronzes was lowered dramatically. Here we report the details of our findings and discuss the formation mechanism.

EXPERIMENTAL

Two different routes of treatment were tested.

I. A 1.296-g amount of H_xMoO_3 (ca. 0.009 mol), which can be prepared from MoO_3 at ambient temperature following the previous procedure (19), was suspended in 30 ml of 0.9 M KCl solution in a Teflon-lined autoclave with a volume of 60 ml stirring on a magnetic stirrer, and then heated in a forced convection oven for certain specified times at 431 K and autogeneous pressure. H_xMoO_3 with various x values was used. Instead of single-phase H_xMoO_3, mixtures of H_xMoO_3 and MoO_3 were also tested. In this case, the mixture ratio of H_xMoO_3 to MoO_3 was calculated in the way, for example, a molybdenum oxide with a H/Mo

---

[1] To whom correspondence should be addressed. Fax: + 81-78-803-5672. E-mail: sotani@kobe-u.ac.jp.

molar ratio of 0.3 can be prepared by mixing 42% $H_{0.71}MoO_3$ with 58% MoO_3.

II. A 0.432-g amount of $H_{0.28}MoO_3$ (0.003 mol) was suspended in 30 ml of 0.9 M deaerated KCl solution in the Teflon-lined autoclave and stirred well with a glass rod. Different from route I, all the loading operations here were done in a nitrogen-filled glove box. The autoclave was then heated in an oven for certain specified times at 431 K.

The resulting blue solid was separated by filtration, ground to a fine powder in a mortar, and then washed several times with distilled water using a centrifuge.

Phase identification was accomplished by X-ray powder diffraction (XRD) using a Mac Science MXP3VZ X-ray diffractometer with Cu*K*α radiation. The morphology of the products was examined by scanning electron microscopy (SEM). The composition of the products was analyzed by a Hitachi 180-80 atomic absorption spectrometer using the 313.3-nm line for Mo, 766.5 nm for K, and by the method of Choain and Marion (20). Infrared spectra were measured for the wavenumbers 500–4000 cm^{-1} by using a Perkin Elmer 1600 FT-IR spectrophotometer. Thermal gravimetric analysis was performed on a Mac Science TG–DTA 2010S system under a nitrogen atmosphere at a heating rate of $10\ K \cdot min^{-1}$.

RESULTS AND DISCUSSION

Preparation of the Blue Molybdenum Bronze

The nature of the products was found to depend strongly on the H/Mo molar ratio. Figure 1 shows the XRD patterns of the products obtained by heating the single-phase H_xMoO_3 with $x = 0.25$, 0.28, and 0.31 at 431 K for 48 h using route I. With the increase of the H/Mo molar ratio, the product changes from blue bronze + MoO_3 to red bronze + MoO_3. As expected, the starting hydrogen molybdenum bronze with high oxidation state of Mo (H/Mo > 0.28 in this work) benefits the formation of red bronze. No red bronze forms from the hydrogen molybdenum bronze with low oxidation state of Mo. The products obtained from the mixture of H_xMoO_3 and MoO_3 also depend on the *x* value of the mixed single-phase H_xMoO_3 rather than the H/Mo ratio of the H_xMoO_3/MoO_3 mixture. The mixed hydrogen molybdenum bronze with high oxidation state of Mo leads to the formation of red bronze. For example, the product from the mixture with a H/Mo ratio of 0.25, which is prepared by 22% $H_{1.15}MoO_3$ + 78% MoO_3, gives the XRD pattern of red bronze + MoO_3 instead of blue bronze + MoO_3; the mixture with a H/Mo ratio of 0.25 prepared by 89% $H_{0.28}MoO_3$ + 11% MoO_3 gives a product of blue bronze + MoO_3.

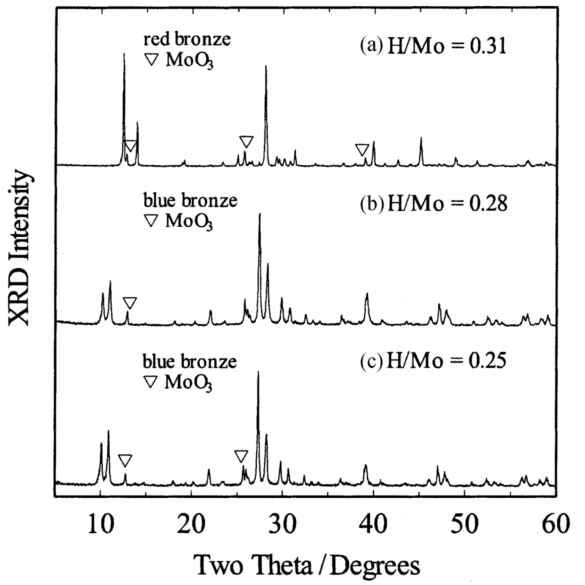

FIG. 1. XRD patterns of the products obtained using H_xMoO_3 with H/Mo ratio of (a) 0.31, (b) 0.28, and (c) 0.25, respectively.

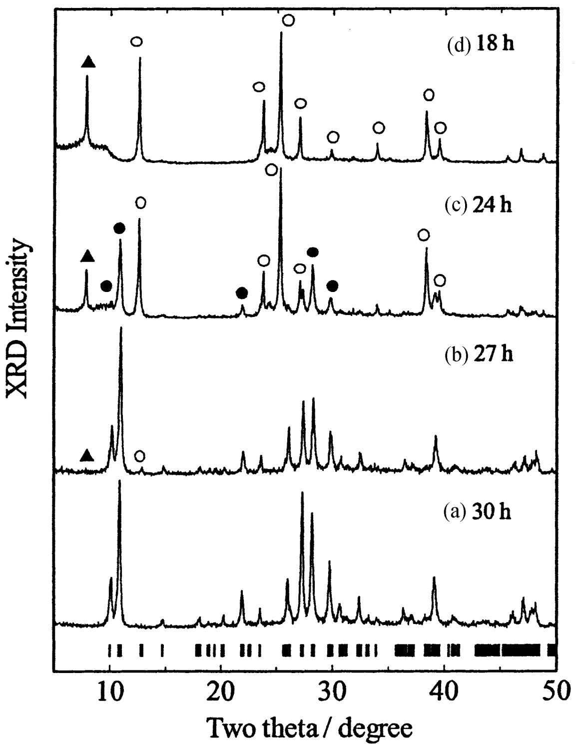

FIG. 2. XRD patterns of the products obtained after heating for (a) 30 h, (b) 27 h, (c) 24 h, and (d) 18 h, respectively. The set of bars at the bottom indicates the positions of reflections from blue bronze calculated by the Rietveld program. Symbols ○, ●, and ▲ indicate H_xMoO_3, blue bronze, and the unidentified phase, respectively.

The formation of the MoO_3 was considered to be the result of the oxidation of the material by air in the autoclave during treatment. We confirmed this by substitution of N_2 for the air, using synthesis route II. Single-phase $H_{0.28}MoO_3$ was chosen as the starting solid to prepare single-phase molybdenum bronze. Figure 2a shows the

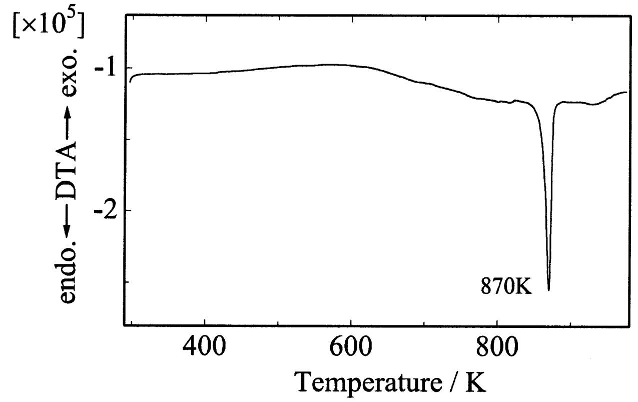

FIG. 3. DTA curve of the blue bronze prepared.

XRD pattern of the product after the hydrothermal treatment in deaerated KCl solution for 30 h under a nitrogen atmosphere. The weight of the loading hydrogen molybdenum bronze is 0.432 g. It will be explained later why the lower weight is better for the preparation of single-phase blue bronze. The pattern agreed well with that of the single-phase blue potassium molybdenum bronze reported in the literature (JCPDS No. 35-444). All the peaks were confirmed to be due to the blue potassium molybdenum bronze calculated by the Rietveld program "Rietan" (21).

The DTA curve of the product (Figure 3) shows one sharp endothermic peak at 870 K, giving the melting point of the obtained blue bronze. No characteristic peaks (22) due to the dehydration before 400 K is observed, which suggests no hydrate water molecules are combined with the alkali metal ions.

The infrared spectrum of the product between the wavenumbers 700–1300 cm^{-1} is shown in Fig. 4. No bands belonging to other molybdenum oxides were found in the spectrum. And no discernible Mo–O–H bands were present, which indicates no hydrogen insertion in the intralayers of the MoO_6 octahedra. The infrared spectra of potassium molybdenum bronzes K_xMoO_3 with variable values of x have been measured by Hirata and Yagisawa (23). The spectra of our work closely resemble those of $K_{0.2}MoO_3$ and $K_{0.3}MoO_3$ prepared by Hirata and Yagisawa except that the MoO_3 bands observed in their spectra are missing in our samples.

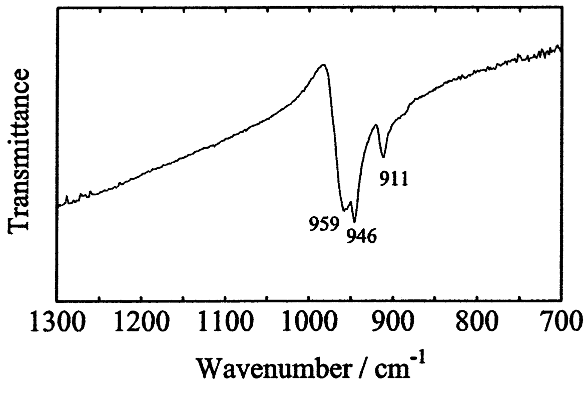

FIG. 4. IR spectra of the blue bronze prepared.

As observed by SEM, the obtained blue bronze was composed of small needle-shaped crystallites with a size of ca.0.1 × 0.1 × 4 μm^3 (Fig. 5e). The oxidation number of Mo in the product was determined to be 5.72, which is the same as that of the starting $H_{0.28}MoO_3$.

The results described above show that the single-phase blue potassium molybdenum bronze, $K_{0.28}MoO_3$, was synthesized at 431 K by the hydrothermal reaction in an oxygen-free autoclave. It also indicates that the as-prepared product was well sheltered from oxidation by oxygen during the hydrothermal reaction.

Formation Process of the Blue Bronze

To gain some insight into the evolution of the molybdenum compounds formed during the hydrothermal reaction, the solid products formed at different stages by synthesis route II were examined by X-ray diffraction. Figure 2d shows the XRD pattern of the product collected after hydrothermal reaction for 18 h in a nitrogen-filled autoclave, which consists of reflection peaks due to H_xMoO_3 and additional peaks marked by black triangles. Figure 2c shows the product obtained by hydrothermal treatment for 24 h. Peaks due to the blue bronze, H_xMoO_3, and the phase marked by black triangles were found in this pattern. The 27-h-heated product is shown in Fig. 2b. The main phase is blue bronze with traces of the phase marked by a black triangle and hydrogen bronze. After 30 h of reaction, the solid shows XRD peaks of a single-phase potassium molybdenum bronze (Fig. 2a). It seems that the conversion of hydrogen molybdenum bronze to blue bronze proceeds through an intermediate phase, which is marked by black triangles in Figs. 2b, 2c, and 2d. The peak at 7.9 marked by a black triangle is very similar to the (020) reflection peak of AD type (air-dried) hydrated potassium molybdenum bronze (24, 25).

In order to ascertain the nature of the unknown phase, TG–DTA measurements were carried out on the 18-h hydrothermally treated sample under a nitrogen flow, as shown in Fig. 6. The endothermic peak appearing at 350.9 K is accompanied by a weight loss corresponding to dehydration. The peak at 7.9° in the XRD of the original phase (see Fig. 2d) marked by black triangles shifts to about 9.0° after heat treatment at 424 K. The shift in the peak position characterizes the change from the AD hydrated molybdenum bronze to VD type (vacuum-dried) bronze (24) during the dehydration process. The next exothermic peak at 599.1 K coinciding with a sharp weight loss was due to the phase decomposition of hydrated molybdenum bronze, in which hydrogen was removed as water molecules with oxygen atoms located in the framework of molybdenum oxide. According to the XRD analysis, the product heated at 683 K was found to consist of blue bronze, MoO_2, and MoO_3. The three phases were the usual products of the hydrogen co-inserted hydrated potassium molybdenum bronze and hydrogen molybdenum bronze after heat treatment in an air-free atmosphere (22, 26–29). On the basis of previous findings, it is reasonable to conclude that the unknown intermediate formed in the hydrothermal reaction was a hydrogen co-inserted AD type hydrated potassium molybdenum bronze, $(K \cdot nH_2O)_YH_xMoO_3$.

To further verify our deduction, hydrothermal treatment was conducted using VD type hydrated potassium molybdenum bronze as the starting material under the same conditions as those in the case of hydrogen molybdenum bronze. A 0.456 g amount of $K_{0.25}MoO_3 \cdot 0.46H_2O$ (VD type), which was prepared following the method of cation exchange (22, 29), was hydrothermally heated in 30 ml of

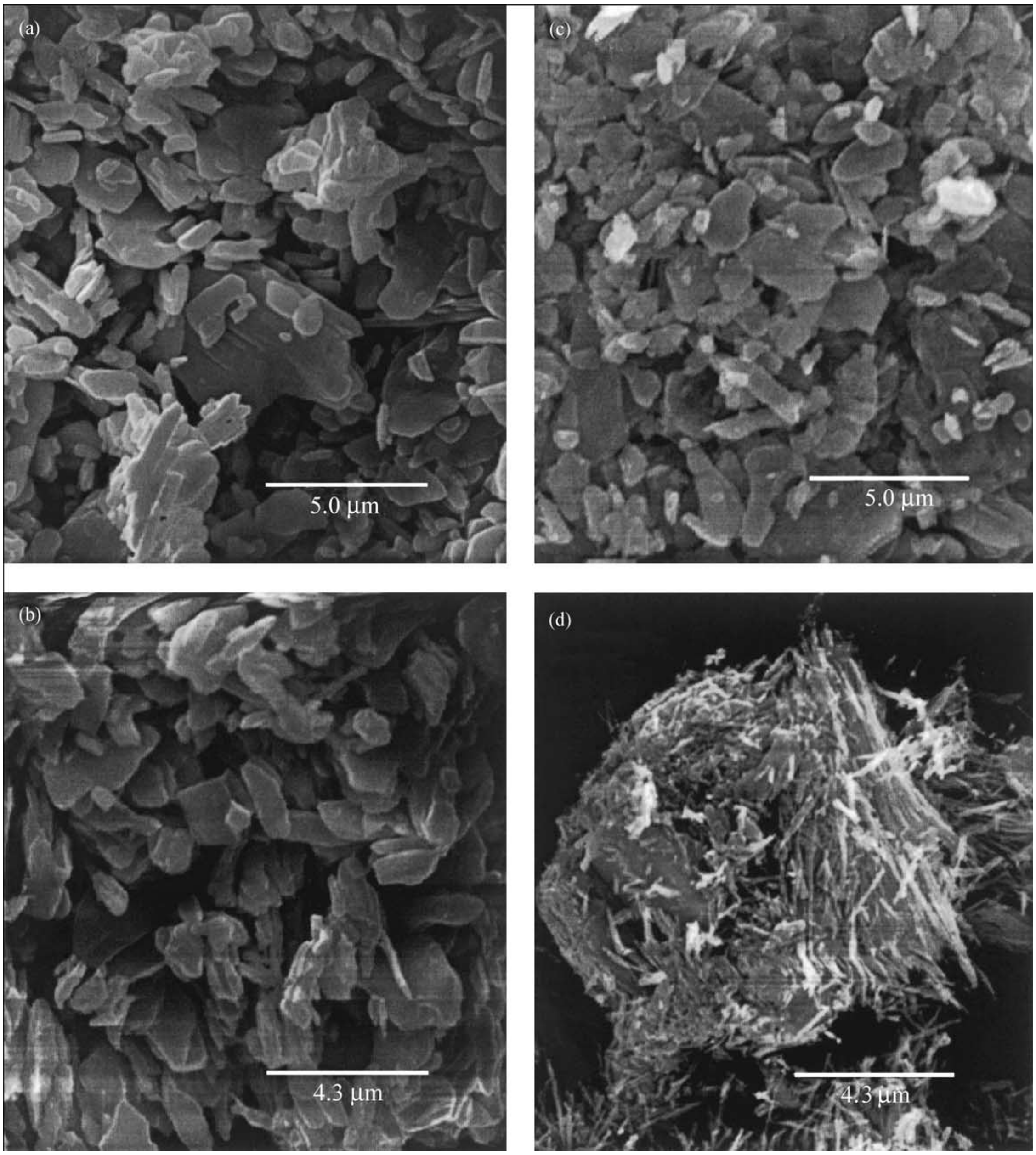

FIG. 5. SEMs of (a) the starting $H_{0.28}MoO_3$, (b) the product formed after 18 h of heating, (c) the hydrate bronze, (d) the product formed after 24 h of heating, and (e) the blue bronze formed after 30 h of heating.

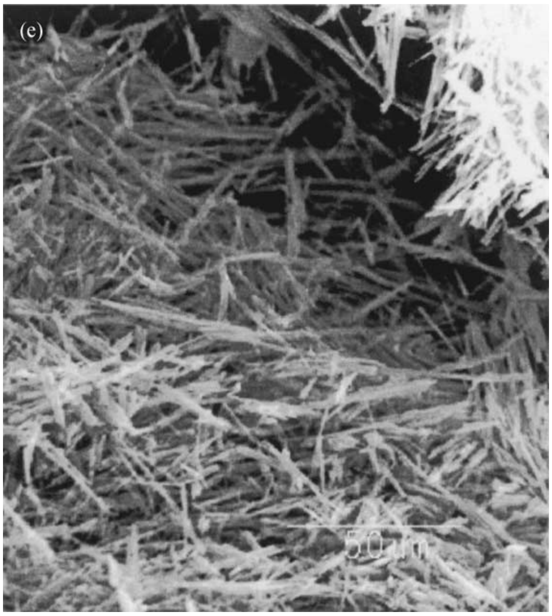

FIG. 5—*Continued*

0.9 M deaerated KCl solution. Figure 7 shows the XRD patterns of the starting VD type bronze and the obtained products. After 14 h of hydrothermal treatment, the (020) peak of the starting VD type bronze shifts to 7.9° (Figs. 7a and 7b), which is of the same degree as that marked by a black triangle in Fig. 2. This expansion of the interlayer spacing should result from the insertion of more water molecules hydrated to the potassium ions under hydrothermal conditions, which caused the VD type bronze to change to the AD type. The formation of both blue bronze and red bronze can be observed in the 18-h product (Fig. 7c). The product collected after 20 h of heating is a mixture of blue bronze and red bronze (Fig. 7d), and remains as a biphasic compound after 30 h of heating. This experiment did not bring out a single-phase blue bronze, though, as described previously, the single-phase blue bronze can be obtained using hydrogen molybdenum bronze as the starting material. In the latter case, the hydrogen bronze remains throughout the whole reaction process until the final formation of the single-phase blue bronze. This fact implies that the hydrogen molybdenum bronze may play as an important role in the formation of the single-phase blue bronze through the hydrogen co-inserted hydrated potassium molybdenum bronze. It is possible that the hydrogen co-inserted molybdenum bronze derived from hydrogen bronze has a unique structure and composition compared with the one from hydrated molybdenum bronze. Or, the slow rate of formation and low-concentration source of hydrogen co-inserted hydrated molybdenum bronze during the heating process of hydrogen bronze may be critical conditions for a complete transformation from hydrogen co-inserted hydrated bronze to anhydrous blue bronze. In summary, the conversion of the solid material during the hydrothermal reaction in an oxygen-free autoclave can be

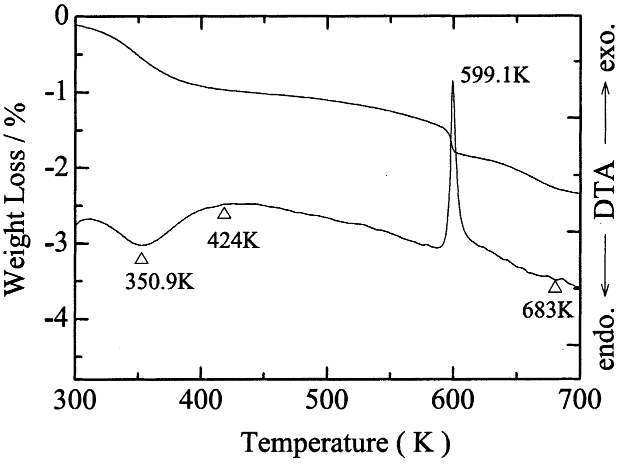

FIG. 6. TG–DTA scans of the product collected after 18 h of hydrothermal reaction.

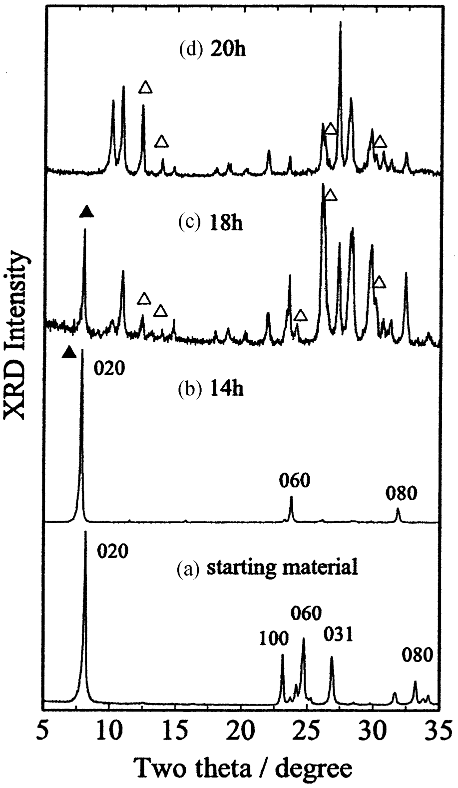

FIG. 7. XRD patterns of (a) the starting hydrated molybdenum bronze and the products after heating for (b) 14 h, (c) 18 h, and (d) 20 h, respectively. Symbols △ and ▲ indicate red bronze and unidentified phase, respectively. All the unlabeled peaks in (c) and (d) are attributed to blue bronze.

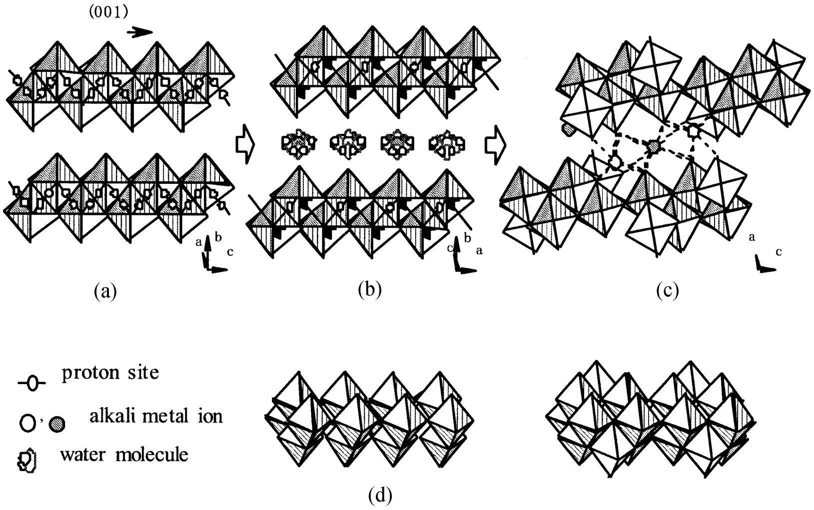

FIG. 8. Structure projections of (a) hydrogen molybdenum bronze, H_xMoO_3 ($0.23 < x < 0.4$), along (100); (b) hydrated molybdenum bronze $(K\cdot nH_2O)_YMoO_3$, along (001); (c) blue molybdenum bronze along (010); (d) trioxide layer along (100); and (e) interlooking $Mo_{10}O_{30}$ units of the blue bronze.

concluded as

$$H_{0.28}MoO_3 \xrightarrow{\text{KCl soln.}} H_xMoO_3$$

$$+ K_yH_zMoO_3\cdot nH_2O \xrightarrow{\text{KClsoln.}} K_{0.28}MoO_3.$$

Since it is not feasible for us to conduct studies of the solid–solution interface and of the solution species that are formed during the hydrothermal reaction, we cannot obtain the exact information needed to establish a detailed reaction mechanism. However, the similarity between the structures of hydrogen molybdenum bronze, hydrated bronze and blue bronze gives us a basis for understanding the formation chemistry.

Figures 8a, 8b, and 8c show the structure projection of hydrogen molybdenum bronze along (001), hydrogen co-inserted hydrated potassium molybdenum bronze along (010), and blue bronze along (010), respectively. Parts of the trioxide layers along (100), and that of the blue bronze along (001), are shown in Figs. 8d and 8e, respectively. It is clear that there is a strong affiliation between these crystal structures. They are all constructed of the same infinite zigzag chains of MoO_6 octahedra, and the whole framework of the trioxide structure is preserved from the hydrogen molybdenum bronze to hydrated bronze except for a small shift of the MoO_3 layers along (001). Figures 5a and 5b show, respectively, the SEM pictures of the starting hydrogen molybdenum bronze, and the 18-h hydrothermally treated product, which is a mixture of hydrogen bronze and hydrated bronze. For comparison, the picture of the single-phase VD type hydrated molybdenum bronze is shown in Fig. 5c. They are all of platelike configurations. No discernible differences in the size and appearance between these three products were observed. It is speculated that, at the initial stage of the hydrothermal reaction, the hydrogen inserted hydrated molybdenum bronze is formed by the topotactical insertion of the hydrated potassium ions into the empty interlayers of hydrogen molybdenum bronze. The stacked trioxide layers, held together by van der Waals forces, might become rather loose under the hydrothermal conditions. Figure 5d shows the SEM picture of the 24-h-treated sample. The right side of the picture shows a bundle of needle-shaped crystallites, which we speculate are stacked layers of hydrated bronze that has almost finished the splitting process. We believe that the splitting originated from the internal rearrangement of the chains of MoO_6 octahedra. By further hydrothermal treatment, the trioxide chains slide along the (001), see Fig. 8b, and initiate the rearrangement as shown in Fig. 8c. Meanwhile, the hydrate water molecules and hydrogens may be "pressed" out during the process. The splitting may have occurred between the interfaces of the newly formed blue bronze crystallites and the hydrogen inserted hydrated bronze. Therefore, we speculate that the conversion from hydrogen bronze to blue bronze proceeds via a solid-state transformation mechanism. The size and morphology of the blue bronze crystallites, which are obtained after 120 h of heating, do not show any differences from those formed in a 30 h heating. This means no crystal growth occurs after 30 h of heating. Other supporting evidence comes from the experiments that we carried out in air-free circumstances using 1.296 g (0.009 mol) of $H_{0.28}MoO_3$ as the starting charge. The product prepared was an inhomogeneous compact block.

Measured by XRD, the sample scraped from the upper surface (the surface contacting with the solution) was single-phase blue bronze, while much MoO_3 formed in the bottom portion of the product, where there was a lack of intimate contact between the hydrogen molybdenum bronze and the KCl solution. The problem could be solved by agitation, or, as we do in synthesis route II, by reducing the amount of starting solid material to such a level that sufficient infiltration of KCl solution could be maintained throughout the reaction. The dissolution/recrystallization mechanism cannot account for this phenomenon. In a dissolution/recrystallization reaction, the solid reagent would keep dissolving in the solution while the crystallites precipitate continuously, thus eliminating the problem of insufficient infiltration.

CONCLUSIONS

Single-phase blue potassium molybdenum bronze was prepared successfully at 431 K in an oxygen-free autoclave by a hydrothermal method, which proved to be an effective and energy-saving way for synthesis. The blue bronze formed from hydrogen molybdenum bronze via an intermediate phase of hydrogen co-inserted hydrated potassium molybdenum bronze under hydrothermal conditions used here.

REFERENCES

1. A. Wold, W. Kunnmann, R. J. Arnott, and A. Ferretti, *Inorg. Chem.* **3,** 545 (1964).
2. D. S. Perloff, M. Vlasse, and A. Wold, *J. Phys. Chem. Solids*, *Suppl.* **1,** 361 (1967).
3. M. H. Whangbo and L. F. Schneemeyer, *Inorg. Chem.* **25,** 2424 (1986).
4. M. Greenblatt, *Chem. Rev.* **88,** 31 (1988).
5. A. Wold, *Bull. Soc. Chim. Fr.* **1965,** 1059 (1965).
6. G. H. Bouchard, J. Perlstein, and M. J. Sienko, *Inorg. Chem.* **6,** 1682 (1967).
7. P. Strobel and M. Greenblatt, *J. Solid state Chem.* **36,** 331 (1981).
8. M. Greenblatt, W. H. McCarroll, R. Neifeld, M. Croft, and J. V. Waszczak, *Solid State Commun.* **51,** 671 (1984).
9. A. Manthiram and J. Gopalakrishnan, *Rev. Inorg. Chem.* **6,** 1 (1984).
10. W. H. McCarroll and M. Greenblatt, *J. Solid State Chem.* **54,** 282 (1984).
11. K. V. Ramanujachary, M. Greenblatt, and W. H. McCarroll, *J. Cryst. Growth* **70,** 476 (1984)
12. C. Tsang, A. Dananjay, J. Kim, and A. Manthiram, *Inorg. Chem.* **35,** 504 (1996).
13. C. F. Tsang and A. Manthiram, *J. Mater. Chem.* **7,** 1003 (1997).
14. K. Eda, K. Furusawa, F. Hatayama, S. Takagi, and N. Sotani, *Bull. Chem. Soc. Jpn.* **64,** 161 (1991).
15. N. Sotani, K. Eda, M. Yanagi-ishi, and S. Takagi, *Mater. Res. Bull.* **28,** 363 (1993).
16. N. Sotani, T. Miyazaki, K. Eda, and F. Hatayama, *J. Mater. Chem.* **7,** 2253 (1997).
17. K. Eda, T. Miyazaki, F. Hatayama, M. Nakagawa, and N. Sotani, *J. Solid State Chem.* **137,** 12 (1998).
18. K. Eda, K. Chin, and M. S. Whittingham, *Chem. Lett.* **8,** 811 (1999).
19. N. Sotani, K. Eda, M. Sadamatsu, and S. Takagi, *Bull. Chem. Soc. Jpn.* **62,** 903 (1989).
20. C. Choain and F. Marion, *Bull. Soc. Chim. Fr.* **1963,** 212 (1963).
21. F. Izumi, *J. Cryst. Soc. Jpn.* **27,** 23 (1985).
22. N. Sotani, T. Suzuki, K. Eda, M. Yanagi-ishi, S. Takagi, and F. Hatayama, *J. Solid State Chem.* **132,** 330 (1997).
23. T. Hirata and K. Yagisawa, *J. Phys.: Condens. Matter.* **2,** 5199 (1990).
24. N. Sotani, K. Eda, and M. Kunitomo, *J. Solid State Chem.* **89,** 123 (1990).
25. K. Eda, A. Sukejima, and N. Sotani, *J. Solid State Chem.* **159,** 51 (2001).
26. D. M. Thomas, *Mater Res. Bull.* **21,** 945 (1986).
27. T. Manago, Master's thesis, Kobe University, 1999.
28. K. Eda, *J. Mater. Chem.* **2**(5), 533 (1992).
29. N. Sotani, T. Manago, T. Suzuki, and K. Eda, *J. Solid State Chem.* **159,** 87 (2001).
30. N. Sotani, Y. Kawamoto, and M. Inui, *Mater. Res. Bull.* **18,** 797 (1983).
31. K. Eda, M. Suzuki, F. Hatayama, and N. Sotani, *J. Mater. Chem.* **7**(5), 821 (1997).